Hindawi
Journal of Advanced Transportation
Volume 2023, Article ID 1689075, 12 pages
https://doi.org/10.1155/2023/1689075

Research Article

Multiparadigm Modeling Framework to Evaluate the Impacts of Travel Patterns on Electric Vehicle Battery Lifespan

Shubham Agrawal,[1] **Srinivas Peeta**,[2,3] **and Mohammad Miralinaghi**[4]

[1]*Department of Psychology, Clemson University, Clemson, SC 29630, USA*
[2]*School of Civil and Environmental Engineering, Georgia Institute of Technology, Atlanta, GA 30332, USA*
[3]*H. Milton Stewart School of Industrial and Systems Engineering, Georgia Institute of Technology, Atlanta, GA 20332, USA*
[4]*Department of Civil, Architectural and Environmental Engineering, Illinois Institute of Technology, Chicago, IL 60616, USA*

Correspondence should be addressed to Shubham Agrawal; agrawa3@clemson.edu

Received 29 December 2021; Revised 10 September 2022; Accepted 5 October 2022; Published 16 February 2023

Academic Editor: Alessandro Severino

The widespread adoption of electric vehicles (EVs) can help attain economic and environmental sustainability by reducing oil dependency and greenhouse gas emissions. However, several issues need to be addressed before EVs can become a popular vehicle choice among the general public. A key issue is the perpetual reduction in EV battery capacity caused by battery degradation over time with usage. This can lead to a reduced driving range and cause "range anxiety" for EV drivers. This becomes even more critical in developing countries where consumers are highly sensitive to battery replacement costs. Thus, to promote EVs in developing economies, policymakers and vehicle manufacturers need to develop attractive incentive schemes and warranty strategies preceded by a thorough assessment of the useable EV battery lifespan for a wide range of users. This paper develops a multiparadigm modeling framework to compute battery degradation for a large population of EVs by capturing the effects of travel patterns, traffic conditions, and ambient temperature. The proposed framework consists of four different building blocks: (i) a microscopic traffic simulation model to generate speed profiles, (ii) an EV power consumption model, (iii) a battery equivalent circuit model, and (iv) a semiempirical battery degradation model. The proposed framework can also be used to assess the battery life-cycle of electric-powered automated vehicles by adjusting their travel patterns accordingly. A case study is presented using travel diary data of around 700 households from the U.S. National Household Travel Survey of 2009 to simulate household travel patterns and corresponding battery lifespan distribution.

1. Introduction

The transportation sector's share of energy consumption has been steadily increasing in developing economies like India [1]. This makes the transportation sector in developing countries one of the major contributors to urban air pollution [2]. Electric vehicles (EVs) have zero tailpipe emissions, making them a promising alternative to conventional fossil fuel-based vehicles for curbing greenhouse gas emissions [3]. EVs can also potentially reduce national oil dependency as the renewable and nuclear energy sectors grow. Several automobile companies have already introduced EVs to the market. For example, in 2021, Volvo announced a plan to cease ICEV production from 2030 onwards and to produce only BEVs and PHEVs [4]. Policymakers are also currently offering incentives to encourage the purchase of EVs [5]. For example, under the clean vehicle rebate project [6], the California Environmental Protection Agency (CalEPA) provides a rebate of up to $7,000 for EV purchases.

Despite international efforts, the greater adoption of EVs still faces several challenges. For example, the reduced maximum driving range due to battery degradation can accentuate range anxiety (i.e., the fear of running out of battery charge before completing the trip) among EV drivers over time [7, 8]. The costs associated with battery replacement from degradation can further deter EV purchases. This

impending inconvenience and economic burden make affordable EVs unattractive for new automobile buyers, especially in developing countries where consumers are more sensitive towards costs. The scarcity of information on battery degradation and contributing factors also plays a critical role in increasing consumer skepticism. A thorough understanding of the effects of travel patterns, driving characteristics, and environmental factors on EV battery lifespan would assist vehicle manufacturers and policymakers in designing appealing incentive schemes and warranty strategies to increase EV adoption [9]. It can also help consumers make informed decisions based on their travel patterns and driving behaviors.

In this context, this study proposes a multiparadigm modeling framework to estimate the useable battery lifespan of a large population of EVs. The useable battery lifespan is defined as the duration within which the maximum EV battery capacity degrades below a certain threshold of its original capacity and needs to be replaced for regular use. It is an important factor in deriving the energy consumption estimation model for EVs [10]. The generally accepted battery degradation threshold before it needs replacement is considered to be 20 to 30% of its original capacity [11, 12]. The proposed modeling framework consists of four different building blocks: (i) a network-level microscopic traffic simulation model to obtain realistic drive cycles or speed profiles (i.e., a series of vehicle speeds versus time) of the vehicles; (ii) an EV power consumption model to compute the power profile from the speed profile; (iii) a battery circuit model that converts the power profile to a battery current flow profile; and (iv) a semiempirical battery degradation model that simulates battery lifespan based on current flows and ambient temperature. The multiparadigm approach provides the flexibility to use the most suitable modeling methods at each step. Some studies have used multiparadigm or multistage approaches in EV-related research, including digital battery lifespan management [13]; however, to the best of our knowledge, they have not been used to understand the impacts of travel patterns on the battery lifespan.

Battery degradation or battery aging can be classified into two different mechanisms: calendar aging (during storage) and cycle aging (during use). Aging happens as a result of structural disordering, variation in electrolyte composition, or loss of active material caused by thermodynamic instability [14, 15]. Calendar aging is mainly caused by the growth of a protective layer at the anode called solid electrolyte interphase (SEI), which results in the loss of active material (e.g., lithium) and increased electrode impedance [14, 16]. Cycle aging is mainly caused by structural changes and chemical decomposition of active material at the cathode and changes in SEI at the anode from electrolyte reactions during charging and discharging [17]. Although total degradation is considered as the summation of both calendar aging and cycle aging, their degradation mechanisms are not independent, and interactions occur [17]. This study focuses on modeling Li-ion battery degradation since most commercially available EVs use lithium-ion (Li-ion) battery packs [8]. Due to the inherent complexity of aging mechanisms and their interactions, several semiempirical battery degradation models [11, 18–21] and statistical models [22] based on experimental data have been proposed in the past literature.

Several efforts have been made in the past to quantify the useable battery lifespan of EVs. For example, Marano et al. [23] and Onori et al. [24] proposed a model to compute battery degradation for plug-in hybrid electric vehicles (PHEVs) using depth-of-discharge (DoD) (i.e., the percentage of battery capacity used before recharging) and battery temperature using linear combinations of standard driving schedules like the Urban Dynamometer Driving Schedule (UDDS) [25], which limits its applicability to a large population of EVs with diverse travel patterns and driving behavior. Guenther et al. [26] investigated vehicle-to-grid applications for synthetic drive cycles using a simplistic energy-based battery model, which ignores the effects of internal resistance and cell voltage at different state-of-charge (SOC) (i.e., the percentage of battery capacity available). Peterson et al. [27] analyzed vehicle-to-grid applications using UDDS and concluded that using a realistic drive cycle is important to quantify battery degradation as DoD may provide misleading results. Some studies have evaluated the impacts of battery recharging strategies on battery degradation using a combination of DoD, SOC, and/or temperature [28, 29]. However, these models assume a very simplistic drive cycle with little or no variation in speed and, hence, the current flow through the battery. Remmlinger et al. [30] presented a method to compute the degradation index relative to the degradation of new batteries by using the measurement values of cell voltage and current flow. Pelletier et al. [31] provide a brief overview of several Li-ion battery degradation models that can be used for EV applications. The proposed multiparadigm framework extends the existing battery lifespan computation frameworks by introducing a microscopic simulation layer to assess heterogeneity in travel patterns and driving behavior. Yang et al. [32] developed a novel analytical framework to determine battery degradation based on travel demand and the ambient high temperature of the battery. Their results show that battery life ranges from approximately 5 years in Florida to 13 years in Alaska, the United States. They also showed that if an EV continues to operate after the 30% battery degradation limit, the greenhouse gas emissions and energy consumption can be significantly increased. Xu et al. [33] proposed a Q-learning-based strategy to minimize Li-ion battery degradation and energy consumption. The Q-learning method is an adaptive optimal control algorithm that uses the Bellman equation of dynamic programming. It is shown that Q-learning decreases the battery capacity loss and increases the lifespan by 13-20%. A summary of the literature on battery degradation models is presented in Table 1.

The key contributions of this research are threefold. First, this study proposes a multiparadigm modeling methodology to derive the useable lifespan of battery of a large population of EVs. Second, this study integrates a microscopic traffic simulation model to account for the driving behavior heterogeneity for battery lifespan

Table 1: Summary of the literature on battery degradation models.

Study	Degradation model	Cycle life	Calendar life	Input
Marano et al. [23]	Damage accumulation model	Y	N	Current severity relative to battery size (i.e., C-rate), temperature, DoD, and SOC
Peterson et al. [27]	Integrated driving and energy use profile modeling framework	Y	N	C-rate, discharge power rate, DoD, and driving profile
Remmlinger et al. [30]	Internal resistance dependent degradation model	Y	N	Temperature, SOC, and power demand
Onori et al. [24]	Weighted Ah-throughput model	Y	N	Temperature and DoD
Guenther et al. [26]	Energy-based battery model	Y	Y	Temperature and power demand
Ouyang et al. [34]	Prognostic and mechanistic model	Y	N	C-rate and temperature
Yang et al. [32]	Pseudo two-dimensional battery capacity fading model	Y	Y	Temperature, travel demand, and driving profile
Calearo et al. [35]	Integrated thermal and SOC dynamics model	Y	Y	Temperature and SOC
Motapon et al. [36]	Physical degradation model	Y	N	C-rate, temperature, and DoD
Olmos et al. [37]	Empirical degradation model	N	Y	C-rate, temperature, DoD, and SOC
Xu et al. [33]	Control-oriented cycle-life model	Y	Y	C-rate, temperature, and SOC
Our study	Semiempirical traffic simulation-based degradation model	Y	Y	C-rate, temperature, travel demand, and driving profile

estimation. Third, each component of the multiparadigm method offers the flexibility to incorporate even newer models or real-world data without changing the framework's overall structure. For instance, real-world vehicle speed data, if available, can replace the traffic simulation model.

The following section introduces the multiparadigm modeling framework to quantify battery lifespan for a large population of EVs and discusses each building block in detail. Then, a case study for the city of Indianapolis, U.S., is presented, and the results are discussed to illustrate the impacts of travel patterns, driving behavior, and temperature on battery lifespan. The paper concludes with a discussion on potential applications of the proposed framework and insights for policymakers, vehicle manufacturers, and other stakeholders to aid greater EV adoption.

2. Methodology: Multiparadigm Modeling Framework

The proposed framework is composed of four modeling stages. This framework requires household vehicle travel patterns as input, which can be obtained using resources such as the U.S. National Household Travel Survey [38]. At a minimum, household vehicle travel patterns should include details about departure time, travel time, and distance traveled for all trips made by a particular vehicle on a given day. The microscopic traffic simulation model based on a real-world road network is calibrated using available traffic demand data to generate realistic drive cycles. Each trip in household travel patterns is then matched to a suitable drive cycle generated by the traffic simulation model. The speed profiles are then fed into an EV power consumption model to compute the power profiles. A battery equivalent circuit model is then employed to get a time series of current flow and SOC of the EV battery. These data are subsequently inputted to a semiempirical battery degradation model to calculate the battery state-of-health (SOH) (i.e., the ratio of current battery capacity to its original capacity).

2.1. Microscopic Simulation Model. Traffic simulation models are widely used to capture nonlinear interactions between vehicles and infrastructure at a microscopic level. Such models can simulate vehicle dynamics and output dynamic variables like position, speed, and acceleration for a large number of vehicles. In this framework, a time series of vehicle speeds is needed to compute the power requirement from the EV battery for propulsion. The simulation model needs to be calibrated using travel demand data between origin-destination pairs for the given road network. The aforementioned information can be gathered from multiple sources, like regional traffic management websites and open-source online resources (e.g., OpenStreetMap). The realism of the simulation model can be further enhanced by including more information such as traffic management infrastructure (e.g., traffic signals) and driver behavior (e.g., car-following model parameters). The simulated drive cycles are then used as input for the EV power consumption model discussed below.

2.2. Electric Vehicle Power Consumption Model. EV power consumption depends directly on the vehicle speed profile. Since the kinetic energy of a vehicle depends on its speed, it is necessary to capture changes in the speed at a microscopic level to accurately compute the vehicle's power requirements. Some simulation packages such as ADVISOR [39] and Autonomie [40] can compute energy consumption and MPGe (miles per gasoline equivalent) using drive cycle data. These tools simulate a detailed EV drivetrain system and hence are computationally expensive. Since a key application

of the proposed framework is to quantify battery degradation for a large population of EVs, it is important to select a computationally efficient model at each step. This study adopts a physical model proposed by Van Haaren [41] to compute power consumption. This approach is used for the following reasons: (i) the model parameters are fitted using real-world Tesla Roadster data [42], and (ii) the computational runtime is significantly lower than the simulation packages mentioned before. This framework provides flexibility to use other similar EV power consumption models that take speed data as a primary input [43, 44].

The physical model used in this study computes the net vehicle power loss/gain (P_{net}) as the sum of two components. First, the power required to maintain a constant speed (P_{cons}). Second, vehicle power requirements at variable speed during loss/gain in kinetic energy while accelerating or braking (P_{kin}). The power loss/gain due to road grade is assumed to be zero but can be added to this model by considering the power gain/loss due to the change in potential energy of the vehicle (P_{pot}). The total power loss (in Watts) at constant speed is the sum of power losses due to aerodynamics (P_{ar}), drivetrain (P_{dr}), rolling friction (P_{rr}), and ancillary systems (P_{an}) as expressed in equations (1)-(6). The parameter definitions and values are presented in Table 2. Some of the parameter values are adapted to match the [43] model, a plug-in electric compact car that accounted for more than 23% of plug-in EV sales in the U.S. in 2013 [45].

$$P_{ar} = \frac{1}{2}\rho A_{veh} C_d V^3, \tag{1}$$

$$P_{dr} = \alpha_{dr} V_{mph}^3 + \beta_{dr} V_{mph}^2 + \gamma_{dr} V_{mph} + c_{dr}, \tag{2}$$

$$P_{rr} = c_{rr} mgV, \tag{3}$$

$$P_{anc} = 180, \tag{4}$$

$$P_{pot} = mg(V \sin\theta), \tag{5}$$

$$P_{cons} = P_{ar} + P_{dr} + P_{rr} + P_{an} + P_{pot}. \tag{6}$$

The total kinetic energy (in Joules) of the vehicle (E_{kin}) consists of linear kinetic energy (E_{lin}) and rotational kinetic energy (E_{rot}). For simplicity, the model assumes that the rotational kinetic energy is approximately 5% of the linear kinetic energy. The power loss/gain at variable speed is the change in kinetic energy (ΔE_{kin}) for the given time interval (Δt) as expressed in equations (7)-(9).

$$E_{lin} = \frac{1}{2} mV^2, \tag{7}$$

$$E_{kin} = E_{lin} + E_{rot} \cong 1.05\, E_{lin}, \tag{8}$$

$$P_{kin} = \frac{\Delta E_{kin}}{\Delta t}. \tag{9}$$

The net power loss is multiplied by the battery-to-motor efficiency factor to account for the inefficiencies in electrical to kinetic energy conversion. Similarly, the regeneration efficiency factor is multiplied to account for the energy recuperation from the regenerative braking system in case of net power gain. The net power consumption of EVs is bounded by their battery limits as expressed in equation (10). This framework assumes these limits as −7 kW (P_{min}) and 100 kW (P_{max}).

$$P_{net} = \begin{cases} P_{max}, & \dfrac{(P_{cons} + P_{kin})}{\beta_{eff}} \geq P_{max}, \\ \dfrac{(P_{cons} + P_{kin})}{\beta_{eff}}, & (P_{cons} + P_{kin}) \geq 0, \\ \beta_{rbs}\,(P_{cons} + P_{kin}), & (P_{cons} + P_{kin}) < 0, \\ P_{min}, & \beta_{rbs}\,(P_{cons} + P_{kin}) \leq P_{min}. \end{cases} \tag{10}$$

2.3. Battery Equivalent Circuit Model. Cycle aging primarily depends on the current flow through the battery during charging or discharging (or C-rate). A 1 C rate is defined as the theoretical discharging current drawn from the battery that will discharge the entire battery in an hour at its rated nominal voltage. A 2 C rate implies double the amount of discharging current corresponding to the 1 C rate; that is, it will discharge the battery in half an hour. This framework implements a battery equivalent circuit as illustrated in equations (11)-(16). The parameter values for Reference [46] are obtained from its owner's manual [46] and advanced vehicle testing activity data [47]. Model parameter definitions and values are presented in Table 3. The model uses 1-D lookup tables to get the cell internal resistance $\mathbf{R}_{int}(\mathbf{t})$ during charging/discharging and open-circuit voltage $\mathbf{V}_{OC}(\mathbf{t})$ at different SOC, as illustrated in Figures 1 and 2, respectively. Due to the lack of data, the internal resistance and open-circuit values are assumed to be constant until the battery's end-of-life (EOL). This assumption can be relaxed by using 2-D lookup tables containing internal resistance and open-circuit voltage values with respect to both battery SOC and SOH, if such data are available.

$$V_{cell}(t) = V_{OC}(t) - R_{int}(t) \cdot I_{cell}(t-1), \tag{11}$$

$$P_{chg}^{max}(t) = \frac{-V_{out}^{max}\left(V_{out}^{max} - V_{OC}(t) \cdot N_s\right)}{R_{int}(t)} \cdot N_t, \tag{12}$$

$$P_{dis}^{max}(t) = \frac{V_{out}^{min}\left(V_{OC}(t) \cdot N_s - V_{out}^{min}\right)}{R_{int}(t)} \cdot N_t, \tag{13}$$

$$\widetilde{P}_{out}(t) = \begin{cases} P_{dis}^{max}(t) & P_{out}(t) \geq P_{dis}^{max}(t) \\ P_{out}(t) & P_{dis}^{max}(t) \geq P_{out}(t) \geq P_{chg}^{max}(t), \\ P_{chg}^{max}(t) & P_{out}(t) \leq P_{chg}^{max}(t) \end{cases} \tag{14}$$

Table 2: EV power consumption model parameters.

Parameter	Definition	Value
V	Vehicle speed in meters per second	
V_{mph}	Vehicle speed in miles per hour	
ρ	Air density (kg/m^3)	1.225
A_{veh}	Vehicle front area (m^2)	2.27
C_d	Drag coefficient	0.28
α_{dr}	Drivetrain coefficient 1	0.004
β_{dr}	Drivetrain coefficient 2	0.5
γ_{dr}	Drivetrain coefficient 3	29.3
c_{dr}	Drivetrain coefficient 4	375
c_{rr}	Rolling resistance coefficient	0.0075
m	Vehicle mass (kg)	1520
g	Gravity (m/s^2)	9.81
θ	Road grade	0
Δt	Discrete time step (s)	1
β_{eff}	Battery to motor efficiency	0.85
β_{rbs}	Regeneration efficiency	0.4
P_{max}	Maximum power output (W)	100,000
P_{min}	Minimum power loss or maximum regeneration/recharging power gain (W)	−7,000

Table 3: Battery equivalent circuit model parameters.

Parameter	Definition	Value
N_s	Number of cells in series in each module	96
N_p	Number of parallel modules	2
N_t	Total number of cells in battery pack	192
$V_{OC}(t)$	Cell open-circuit voltage at time t (V)	Using lookup-table
$R_{\text{int}}(t)$	Cell internal resistance at time t (Ω)	Using lookup-table
$I_{\text{cell}}(t)$	Cell current at time t (A)	$I_{\text{cell}}(0) = 0$
$V_{\text{cell}}(t)$	Cell terminal voltage at time t (V)	
$V_{\text{out}}^{\text{min}}$	Minimum battery terminal voltage (V)	336
$V_{\text{out}}^{\text{max}}$	Maximum battery terminal voltage (V)	403.2
$P_{\text{out}}(t)$	Battery power requirement at time t (W)	
$\widetilde{P}_{\text{out}}(t)$	Actual battery power output at time t (W)	
$P_{\text{dis}}^{\text{max}}(t)$	Maximum battery power output while discharging at time t (W)	
$P_{\text{chg}}^{\text{max}}(t)$	Maximum battery power input while charging at time t (W)	
$I_{\text{rate}}(t)$	C-rate at time t	
K_{cell}	Rated cell capacity (Ah)	33.1
$\delta_{\text{soc}}(t)$	Battery state-of-charge at time t	
δ_{soh}	Battery state-of-health	
Δt	Discrete time step (seconds)	1

$$I_{\text{cell}}(t) = \frac{\widetilde{P}_{\text{out}}(t)}{V_{out}^{c}(t) \cdot N_s} \cdot N_p, \qquad I_{\text{rate}}(t) = \frac{I_{\text{cell}}(t)}{K_{\text{cell}} \cdot \delta_{\text{soh}}}, \tag{15}$$

$$\delta_{\text{soc}}(t) = \delta_{\text{soc}}(t-1) - I_{\text{rate}}(t) \cdot \Delta t. \tag{16}$$

2.4. Battery Degradation Model. Battery degradation is affected by several factors such as battery temperature, SOC, C-rate, and total current throughput (Ah-throughput) [48]. Some models approximate the total Ah-throughput as a product of constant depth-of-discharge and the number of cycles [23]; thereby, ignoring the effects of SOC and C-rate. This framework adopts a semiempirical battery degradation model proposed by Wang et al. [21] that includes three important parameters: time (or battery age), temperature, and C-rate. It computes calendar aging ($\mathbf{Q}_{\text{cal}}$) as a function of time (τ) and temperature ($\mathbf{T}$) and cycle aging ($\mathbf{Q}_{\text{cyc}}$) as a function of temperature, C-rate ($\mathbf{I}_{\text{rate}}$), and lifetime Ah-throughput ($\mathbf{I}_{\text{ah}}$). The model parameters are fitted using experimental aging data for high-power density 1.5 Ah, 18650 cylindrical cells with $\text{LiMn}_{1/3}\text{Ni}_{1/3}\text{Co}_{1/3} + \text{LiMn}_2\text{O}_4$ (NCM + LMO) cathode and a graphite anode. Their results indicate that the predicted values are within ±5% of the measured battery capacity loss. The model can be expressed as equations (17)-(19).

$$Q_T = Q_{\text{cal}} + Q_{\text{cyc}}, \tag{17}$$

$$Q_{\text{cal}} = f\tau^{0.5} \cdot \exp\left(-\frac{E_a}{RT}\right), \tag{18}$$

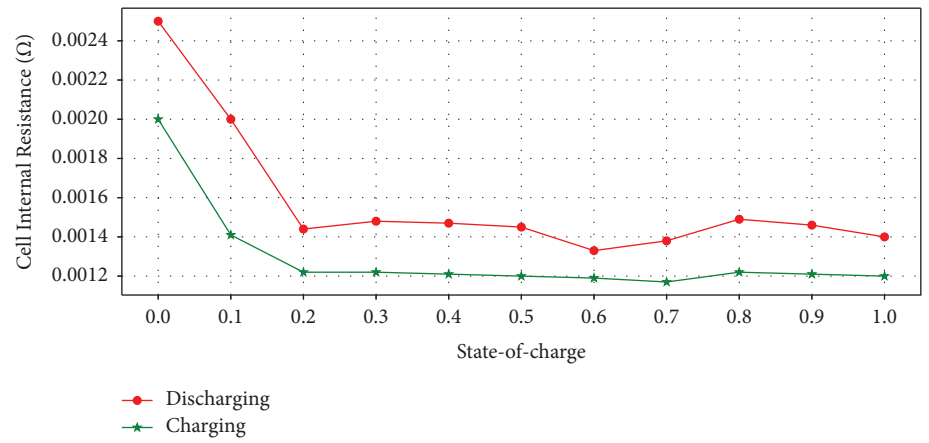

Figure 1: Cell internal resistance values at different SOC.

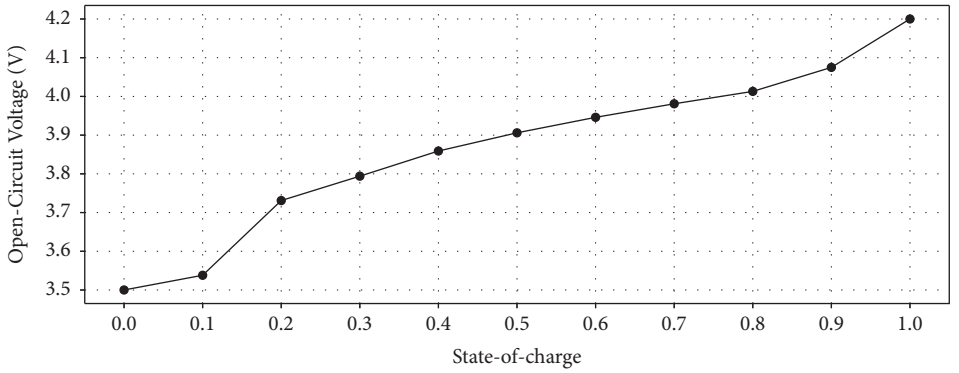

Figure 2: Cell open-circuit voltage values at different SOC.

$$Q_{\text{cyc}} = \left(aT^2 + bT + c\right) \cdot \exp\left[(dT + e) \cdot I_{\text{rate}}\right] \cdot I_{\text{ah}}. \quad (19)$$

To account for the variable C-rate and temperature, the model is modified by taking the differentiating total capacity loss function with respect to a discretized time step ($\Delta\tau$). For each time step, the current flow is assumed to be constant, and instantaneous capacity loss (D_T) is computed as the sum of instantaneous capacity loss D_{cap} and instantaneous cycle loss D_{cyc} by taking the differential of their respective functions. The sum of instantaneous capacity loss is updated to get the total capacity loss until the battery replacement threshold limit (δ_{rep}) is reached. Hence, the battery lifespan is equal to the number of days elapsed before the total capacity loss reaches the specified threshold limit. Because Reference [49] has a rated nominal cell capacity of 33.1 Ah and the data are calibrated for 1.5 Ah cells, a correction factor (β_{corr}) equal to the ratio of rated nominal capacities is multiplied by the cycle loss. Equations (20)-(22) describe the modified model, and Table 4 shows the parameter values.

$$D_T = D_{\text{cal}} + D_{\text{cyc}}, \quad (20)$$

$$D_{\text{cal}} = 0.5\, f\tau^{-0.5} \cdot \exp\left(-\frac{E_a}{\text{RT}}\right), \quad (21)$$

$$D_{\text{cyc}} = \left(aT^2 + bT + c\right) \cdot \exp\left[(dT + e) \cdot I_{\text{rate}}(\tau)\right] \cdot I_{\text{cell}}(\tau) \cdot \beta_{\text{corr}}. \quad (22)$$

This model uses ambient temperature as a proxy for battery temperature, thereby assuming that the thermal effects on internal resistance and cell current are negligible. This assumption can be addressed by including a suitable electrochemical-thermal model in the framework (see Reference [50] for a review) or by using a 1D lookup table to link battery temperature with the environment temperature and battery cell characteristics (e.g., [51, 52]. The model parameters are calibrated for discharging current only. Thus, it is assumed that charging and discharging will have a similar impact on cycle aging based on the absolute value of I_{rate}.

3. Data: Case Study

A case study is presented using the proposed framework for the city of Indianapolis, Indiana, U.S. Real-world household vehicle travel pattern data were extracted from U.S. National Household Travel Survey (NHTS) of 2009 [38]. The NHTS dataset contains 1-day travel diary data of 821 vehicles (with vehicle type as "car") in the state of Indiana. The key variables of the NHTS dataset include household ID, vehicle ID,

Table 4: Battery degradation parameter values and units.

Parameter	Value and unit	Parameter	Value and unit
a	8.61 $e-$ (1/Ah-K^2)	I_{ah}	Lifetime current throughput (Ah)
b	−5.125 $e-$ (1/Ah-K)	$I_{rate}(\tau)$	C-rate at time τ
c	0.7629 (1/Ah)	$I_{cell}(\tau)$	Cell current at time τ (A)
d	−6.7 $e-3$ (1/K-(C-rate))	β_{corr}	1.5/33.1
e	2.35 (1/(C-rate))	E_a	24500 (J/mole)
f	14876 (1/day$^{0.5}$)	R	8.314 (J/K-mole))
τ	Time (in days)	T	Temperature (K)
$\Delta\tau$	Discretized time step (in days)	δ_{rep}	30%

vehicle type, trip departure time, trip arrival time, and trip travel time for all trips made by the household in a single day. Since most affordable EVs have a driving range of about 80-100 miles, vehicles with trip distances exceeding 80 miles for any single trip are excluded from the analysis to avoid situations with EVs running out of battery in the middle of a trip. In the preliminary data analysis, we observed that several vehicles having longer total daily distance did not have sufficient time between trips to recharge the battery. Thus, based on our preliminary data inspection, we also excluded vehicles with total daily distance exceeding 120 miles from the analysis. These distance-based exclusion criteria reduced our dataset to 760 vehicles. A microscopic traffic simulation model is created to generate realistic drive cycles for the vehicles using the simulation software Aimsun [53]. A detailed road network of Indianapolis containing all major freeways, most urban roads, and some minor roads is built in AIMSUN (see Figure 3). A dynamic 15-minute time period origin-destination traffic demand matrix is simulated for a 24-hour time horizon with an additional 1-hour warm-up period. The traffic demand is calibrated using NHTS trip data for Indiana. The departure time period, distance traveled, travel time, and speed profile of each simulated vehicle are recorded. We generated 41,736 unique simulated drive cycles. Each NHTS trip is matched to a simulated drive cycle which has the least Euclidean distance in terms of both trip distance and average speed. NHTS households with missing simulated drive cycle data for any number of trips are excluded from the analysis. Since most affordable EVs have a driving range of about 80-100 miles, vehicles with a trip distance exceeding 80 miles for any single trip or total daily distance exceeding 120 miles are also excluded. In the end, a total of 3,225 trips made by 697 vehicles were analyzed. Most parameter values in the battery equivalent circuit model and degradation model are taken for Reference [43] with a 24 kWh Li-ion battery. The battery degradation threshold is taken as 30%, that is, the battery is considered to be unusable once its SOH is 70%. Daily average temperature values for Indianapolis in the year 2018 (see Figure 4) are used in a loop to compute both calendar and cycle aging [54]. Since degradation computation is performed for each time step, it allows the use of higher resolution temperature data (e.g., hourly temperature) for more accuracy. Due to data limitations, it is assumed that household vehicle travel patterns remain unchanged until the end of useable battery life. This assumption can be relaxed with the availability of a richer travel pattern dataset. The vehicle is assumed to be fully charged to its SOH level at the start of every day. Opportunistic charging behavior is assumed during the day with a constant charging power of 7 kWh.

Figure 3: Road network of Indianapolis, U.S., used in the simulation.

4. Results and Discussion

The impacts of driving behavior and travel patterns on battery lifespan are analyzed using the proposed multi-paradigm modeling framework. Figure 5 shows the daily distance traveled distribution for the case study data. More than 80% of households travel less than 50 miles per day. Using simulated drive cycles allows the analysis of heterogeneity in driving behaviors such as average speed and speed deviation. The average speed and speed deviation for all households' combined daily drive cycles of all trips are illustrated in Figure 6. The population means of average speed and speed deviation are 37.9 mph and 16.4 mph, respectively.

Most automobile manufacturers offer battery warranties based on either battery age, total distance traveled, or their

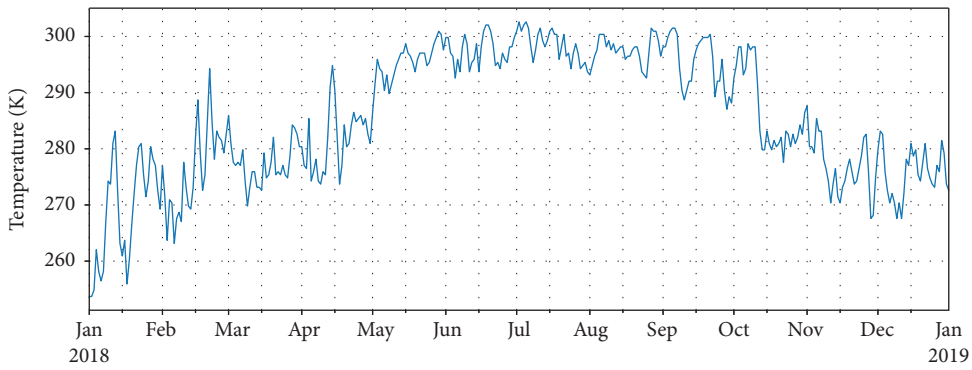

Figure 4: Daily average temperature values for Indianapolis, U.S., in 2018.

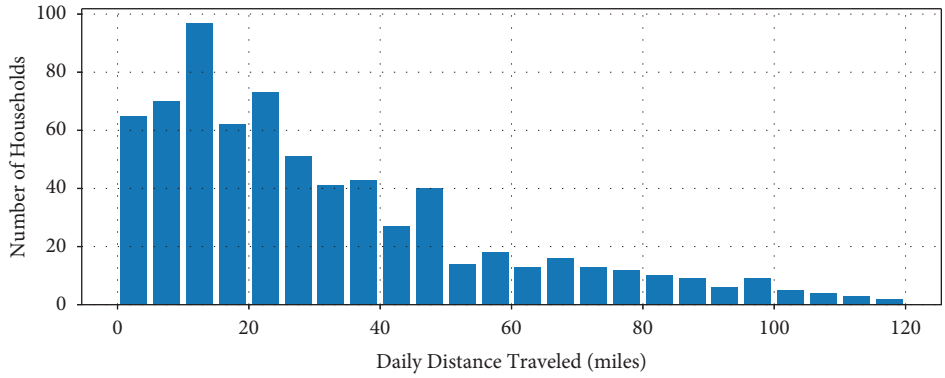

Figure 5: Daily distance traveled distribution.

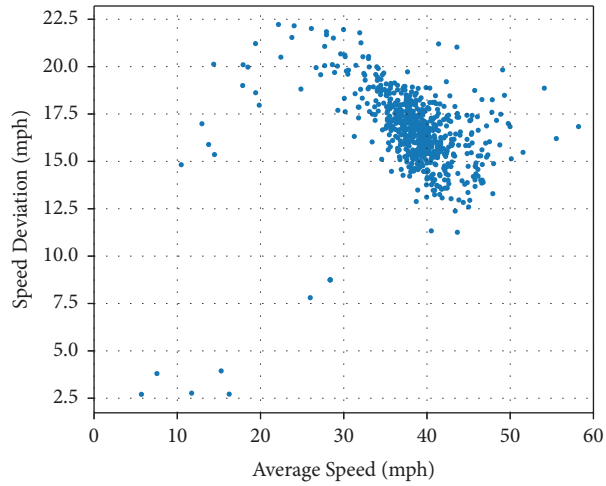

Figure 6: Speed deviation vs. average speed for combined daily drive cycles of households.

combination as a threshold. For example, Reference [46] covers the necessary repairs needed to return battery capacity to about 75% of the original capacity for a period of 5 years or 60,000 miles, whichever comes first [49]. The case study analysis results indicate that almost 50% of the batteries reach their SOH threshold within 5 years and 90% within 8 years. The useable battery lifespan distribution is illustrated in Figure 7. In terms of total distance traveled before EOL, the 50% and 90% quantiles for battery lifespan are approximately 44,500 miles and 72,500 miles, respectively.

To analyze the impact of driving behavior, the average speed and speed deviation for each household are classified as "higher" or "lower" groups based on their value compared to their respective population means. The results indicate that there is little or no difference between the higher and lower average speed groups for the same total distance traveled before EOL (see Figure 8). On the contrary, an

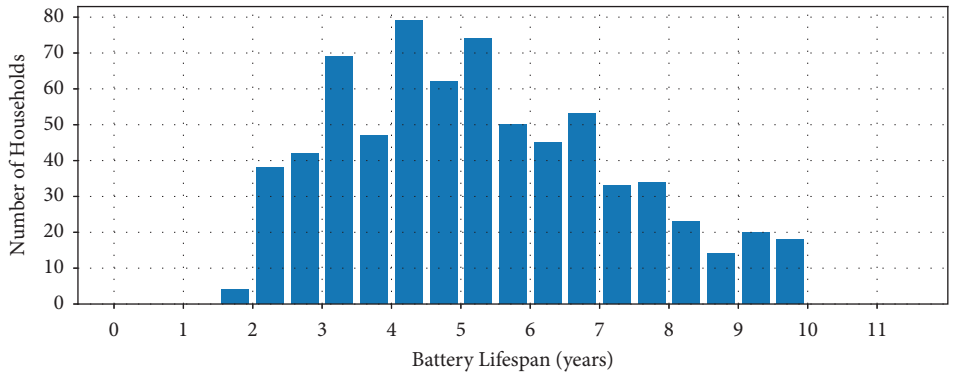

Figure 7: Useable battery lifespan distribution.

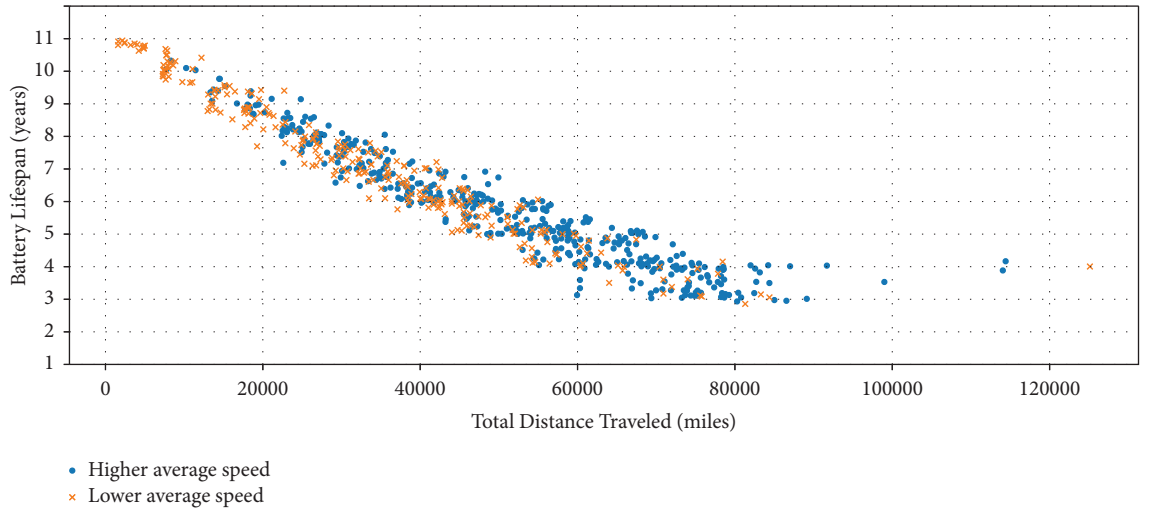

Figure 8: Battery lifespan vs. total distance traveled for average speed-based classification.

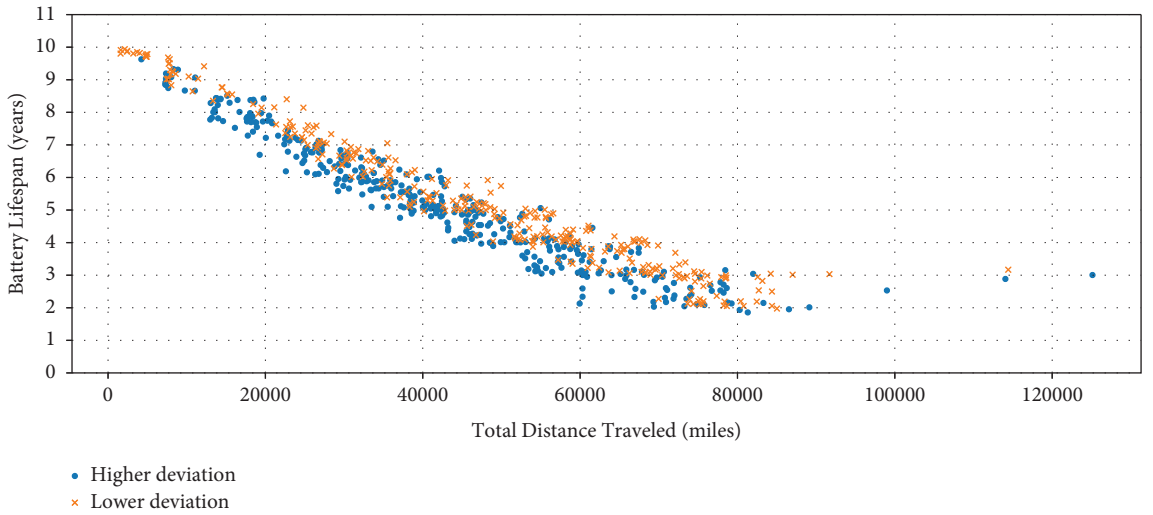

Figure 9: Battery lifespan vs. total distance traveled for speed deviation-based classification.

apparent decrease in battery lifespan can be observed among households with higher speed deviation than those of lower speed deviation (see Figure 9). A higher speed deviation entails more fluctuations in kinetic energy due to acceleration and deceleration (see Section 2.2), which increases the vehicle's overall power consumption. Hence, the difference in lifespan is caused by this additional amount of power required, and thereby, the current flows through the battery to balance the fluctuating kinetic energy at variable speed. These findings illustrate the importance of using realistic and

diverse drive cycles over combinations of standard driving schedules to account for differences in driving behaviors.

5. Concluding Comments

This study presents a multiparadigm modeling framework to quantify the useable battery lifespan of a large population of EVs. The inclusion of a microscopic traffic simulation model in the framework enables the analysis of driving behavior heterogeneity in battery lifespan estimation. Each building block of the multiparadigm approach provides the flexibility to include newer models or real-world cases without affecting the framework structure. For example, the traffic simulation model can be replaced by real-world vehicle speed data if such data are available. This study uses the vehicle and battery specifications of Reference [49] in the case study, but the proposed framework can be used to assess other EVs, such as e-rickshaws, by changing the parameter values accordingly. The impacts of vehicle travel patterns and driving behavior (e.g., speed deviation) on EV battery lifespan under regional temperature trends can provide useful information for vehicle owners, policymakers, and vehicle manufacturers. The framework can be used by vehicle owners to assess the lifetime cost of EV ownership, including battery maintenance cost, insurance cost, and battery resale value, based on their travel needs, driving behavior, and geographic location. In addition, policymakers can use battery lifespan distribution for regional temperature and traffic conditions to design incentive strategies, such as tax credits and extended battery warranties, to regulate EV adoption trajectories. It allows vehicle manufacturers to factor in regional conditions and consumer driving behaviors while evaluating the performance and economics of different batteries by modifying the battery equivalent circuit model and degradation model accordingly. The proposed framework can be utilized to enhance EV research applications such as battery management strategies (e.g., maximum/minimum SOC range) to enhance battery lifespan, battery recharging strategies, vehicle-to-grid applications, etc., by including realistic vehicle travel patterns and driving behavior. Furthermore, there is an ongoing argument among researchers to promote electric-powered autonomous vehicles (AVs) over gasoline-powered AVs to limit greenhouse gas emissions and mitigate negative environmental impacts. The proposed framework can be used to assess the battery life and, thereby, life cycle environmental impacts of a large population of electric-powered AVs. This research can be extended in different directions. The first potential future research direction is to integrate the electrochemical-thermal effects into the battery degradation model. This integration enables for more accurate battery health state monitoring as it accounts for the external measurements of terminal voltage, applied current, and surface temperature of the battery [13, 55, 56]. The second research direction is to compare the effects of travel patterns on fuel consumption between EVs and traditional internal combustion engine vehicles. The third research direction is to consider the battery degradation model for different types of batteries used in EVs. The battery degradation of different EV batteries varies based on the charging/discharging rate, number of cycles, and temperature. The detailed information for some recent battery technology is presented by Zhao et al. [57] and Mathieu et al. [58]. The disaggregate battery degradation model should be calibrated for each type of EV to increase the accuracy of the results.

Data Availability

The data used to support the findings of this study are available on request.

Conflicts of Interest

The authors declare that they have no conflicts of interest.

Acknowledgments

This work was supported as part of the NEXTRANS Center Region 5 University Transportation Center funded by the U.S. Department of Transportation. Any errors or omissions remain the sole responsibility of the authors. [grant number NEXTRANS Center].

References

[1] U.S. Energy information administration, *Country Analysis Executive Summary*, India, 2020.

[2] U.S. Environmental protection agency, *Inventory of U.S. Greenhouse Gas Emissions and Sinks 1990-2019*, 2021.

[3] U.S. Department of energy, "Alternative Fuels Data Center: Emissions from Hybrid and Plug-In Electric Vehicles," 2021, https://afdc.energy.gov/vehicles/electric_emissions.html.

[4] J. Ewing, *Volvo Plans to Sell Only Electric Cars by 2030*, Springer, Berlin, 2021.

[5] M. Miralinaghi and S. Peeta, "Promoting zero-emissions vehicles using robust multi-period tradable credit scheme," *Transportation Research Part D: Transport and Environment*, vol. 75, 2019.

[6] Air resources board, *Implementation Manual for the Clean Vehicle Rebate Project (CVRP)*, 2021.

[7] S. Agrawal, H. Zheng, S. Peeta, and A. Kumar, "Routing aspects of electric vehicle drivers and their effects on network performance," *Transportation Research Part D: Transport and Environment*, vol. 46, pp. 246–266, 2016.

[8] NITI aayog, & world energy council, *Zero Emission Vehicles (ZEVS): Towards a Policy Framework*, 2018.

[9] S. Hasan, "Assessment of electric vehicle repurchase intention: a survey-based study on the Norwegian EV market," *Transportation Research Interdisciplinary Perspectives*, vol. 11, Article ID 100439, 2021.

[10] H. Wang, D. Zhao, Y. Cai, Q. Meng, and G. P. Ong, "A trajectory-based energy consumption estimation method considering battery degradation for an urban electric vehicle network," *Transportation Research Part D: Transport and Environment*, vol. 74, pp. 142–153, 2019.

[11] E. Sarasketa-Zabala, I. Gandiaga, L. M. Rodriguez-Martinez, and I. Villarreal, "Calendar ageing analysis of a LiFePO 4/graphite cell with dynamic model validations: towards realistic lifetime predictions," *Journal of Power Sources*, vol. 272, pp. 45–57, 2014.

[12] S. Saxena, C. Le Floch, J. MacDonald, and S. Moura, "Quantifying EV battery end-of-life through analysis of travel needs with vehicle powertrain models," *Journal of Power Sources*, vol. 282, pp. 265–276, 2015.

[13] S. Yang, R. He, Z. Zhang, Y. Cao, X. Gao, and X. Liu, "CHAIN: Cyber Hierarchy and Interactional Network Enabling Digital Solution for Battery Full-Lifespan Management," *Matter*, no. 3(1), pp. 27–41, 2020.

[14] A. Barré, B. Deguilhem, S. Grolleau, M. Gérard, F. Suard, and D. Riu, "A review on lithium-ion battery ageing mechanisms and estimations for automotive applications," *Journal of Power Sources*, vol. 241, pp. 680–689, 2013.

[15] M. Broussely, P. Biensan, F. Bonhomme et al., "Main aging mechanisms in Li ion batteries," *Journal of Power Sources*, vol. 146, no. 1–2, pp. 90–96, 2005.

[16] R. B. Wright, C. G. Motloch, J. R. Belt et al., "Calendar- and cycle-life studies of advanced technology development program generation 1 lithium-ion batteries," *Journal of Power Sources*, vol. 110, no. 2, pp. 445–470, 2002.

[17] J. Vetter, P. Novak, M. R. Wagner et al., "Ageing mechanisms in lithium-ion batteries," *Journal of Power Sources*, vol. 147, no. 1–2, pp. 269–281, 2005.

[18] D. Le and X. Tang, "Lithium-ion battery state of health estimation using Ah-V characterization," *Annual Conference of the Prognostics and Health Management Society*, pp. 1–7, 2011.

[19] E. Sarasketa-Zabala, I. Gandiaga, E. Martinez-Laserna, L. M. Rodriguez-Martinez, and I. Villarreal, "Cycle ageing analysis of a LiFePO 4/graphite cell with dynamic model validations: towards realistic lifetime predictions," *Journal of Power Sources*, vol. 275, pp. 573–587, 2015.

[20] J. Wang, P. Liu, J. Hicks-Garner et al., "Cycle-life model for graphite-LiFePO4 cells," *Journal of Power Sources*, vol. 196, no. 8, pp. 3942–3948, 2011.

[21] J. Wang, J. Purewal, P. Liu et al., "Degradation of lithium ion batteries employing graphite negatives and nickel-cobalt-manganese oxide + spinel manganese oxide positives: Part 1, aging mechanisms and life estimation," *Journal of Power Sources*, vol. 269, pp. 937–948, 2014.

[22] E. V. Thomas, I. Bloom, J. P. Christophersen, and V. S. Battaglia, "Statistical methodology for predicting the life of lithium-ion cells via accelerated degradation testing," *Journal of Power Sources*, vol. 184, no. 1, pp. 312–317, 2008.

[23] V. Marano, S. Onori, Y. Guezennec, G. Rizzoni, and N. Madella, "Lithium-ion batteries life estimation for plug-in hybrid electric vehicles," *2009 IEEE Vehicle Power and Propulsion Conference*, IEEE, pp. 536–543, September 2009.

[24] S. Onori, P. Spagnol, V. Marano, Y. Guezennec, and G. Rizzoni, "A new life estimation method for lithium-ion batteries in plug-in hybrid electric vehicles applications," *International Journal of Power Electronics*, vol. 4, no. 3, pp. 302–319, 2012.

[25] U.S. Environmental protection agency, *Dynamometer Drive Schedules*, 2017.

[26] C. Guenther, B. Schott, W. Hennings, P. Waldowski, and M. A. Danzer, "Model-based investigation of electric vehicle battery aging by means of vehicle-to-grid scenario simulations," *Journal of Power Sources*, vol. 239, pp. 604–610, 2013.

[27] S. B. Peterson, J. Apt, and J. F. Whitacre, "Lithium-ion battery cell degradation resulting from realistic vehicle and vehicle-to-grid utilization," *Journal of Power Sources*, vol. 195, no. 8, pp. 2385–2392, 2010.

[28] I. J. Fernández, C. F. Calvillo, A. Sánchez-Miralles, and J. Boal, "Capacity fade and aging models for electric batteries and optimal charging strategy for electric vehicles," *Energy*, vol. 60, pp. 35–43, 2013.

[29] B. Lunz, Z. Yan, J. B. Gerschler, and D. U. Sauer, "Influence of plug-in hybrid electric vehicle charging strategies on charging and battery degradation costs," *Energy Policy*, vol. 46, pp. 511–519, 2012.

[30] J. Remmlinger, M. Buchholz, M. Meiler, P. Bernreuter, and K. Dietmayer, "State-of-health monitoring of lithium-ion batteries in electric vehicles by on-board internal resistance estimation," *Journal of Power Sources*, vol. 196, no. 12, pp. 5357–5363, 2011.

[31] S. Pelletier, O. Jabali, G. Laporte, and M. Veneroni, "Battery degradation and behaviour for electric vehicles: review and numerical analyses of several models," *Transportation Research Part B: Methodological*, vol. 103, pp. 158–187, 2017.

[32] F. Yang, Y. Xie, Y. Deng, and C. Yuan, "Predictive modeling of battery degradation and greenhouse gas emissions from U.S. state-level electric vehicle operation," *Nature Communications*, vol. 9, no. 1, pp. 2429–2510, 2018.

[33] B. Xu, J. Shi, S. Li, H. Li, and Z. Wang, "Energy consumption and battery aging minimization using a Q-learning strategy for a battery/ultracapacitor electric vehicle," *Energy*, vol. 229, Article ID 120705, 2021.

[34] M. Ouyang, X. Feng, X. Han, L. Lu, Z. Li, and X. He, "A dynamic capacity degradation model and its applications considering varying load for a large format Li-ion battery," *Applied Energy*, vol. 165, pp. 48–59, 2016.

[35] L. Calearo, A. Thingvad, and M. Marinelli, "Modeling of Battery Electric Vehicles for Degradation Studies," in *Proceedings of the 2019 54th International Universities Power Engineering Conference (UPEC)*, pp. 1–6, IEEE, Bucharest, Romania, September 2019.

[36] S. N. Motapon, E. Lachance, L.-A. Dessaint, and K. Al-Haddad, "A generic cycle life model for lithium-ion batteries based on fatigue theory and equivalent cycle counting," *IEEE Open Journal of the Industrial Electronics Society*, vol. 1, pp. 207–217, 2020.

[37] J. Olmos, I. Gandiaga, A. Saez-de-Ibarra, X. Larrea, T. Nieva, and I. Aizpuru, "Modelling the cycling degradation of Li-ion batteries: chemistry influenced stress factors," *Journal of Energy Storage*, vol. 40, Article ID 102765, 2021.

[38] F. Highway Administration, *National Household Travel Survey of 2009*, Springer, Berlin, 2010.

[39] National renewable energy laboratory, *ADVISOR Advanced Vehicle Simulator*, 2003.

[40] Argonne national laboratory, *Autonomie*, 2016.

[41] R. Van Haaren, "Assessment of electric cars' range requirements and usage patterns based on driving behavior recorded in the National Household Travel Survey of 2009," *U.S. Energy Information Administration*, vol. 1, no. 917, 2011.

[42] J. B. Straubel, "Roadster Efficiency and Range," *Tesla Motors*, 2008.

[43] J. G. Hayes and K. Davis, "Simplified electric vehicle powertrain model for range and energy consumption based on EPA coast-down parameters and test validation by Argonne National Lab data on the Nissan Leaf," in *Proceedings of the 2014 IEEE Transportation Electrification Conference and Expo (ITEC)*, pp. 1–6, IEEE, Dearborn, MI, USA, June 2014.

[44] X. Wu, D. Freese, A. Cabrera, and W. A. Kitch, "Electric vehicles' energy consumption measurement and estimation," *Transportation Research Part D: Transport and Environment*, vol. 34, pp. 52–67, 2015.

[45] U.S. Department of energy, "Alternative Fuels Data Center," *Maps and Data—U.S. Plug-in Electric Vehicle Sales by Model*, 2018, https://afdc.energy.gov/data/10567.

[46] Nissan, *Leaf Owner's Manual*, 2013, https://owners.nissanusa.com/content/techpub/ManualsAndGuides/NissanLEAF/2013/2013-NissanLEAF-owner-manual.pdf.

[47] Idaho national laboratory, *Advanced Vehicle Testing Activity INL/MIS-11-22490*, https://doi.org/INL/MIS-11-22490, 2016.

[48] D. Magnor, J. B. Gerschler, M. Ecker, P. Merk, and D. U. Sauer, "Concept of a Battery Aging Model for Lithium-Ion Batteries Considering the Lifetime Dependency on the Operation Strategy," in *Proceedings of the 24th European Photovoltaic Solar Energy Conference*, pp. 21–25, September 2009.

[49] Nissan, *2013 Leaf Warranty Information Booklet*, 2013, https://owners.nissanusa.com/content/techpub/ManualsAndGuides/LEAF/2013/2013-LEAF-warranty-booklet.pdf.

[50] J. Jaguemont, L. Boulon, and Y. Dubé, "A comprehensive review of lithium-ion batteries used in hybrid and electric vehicles at cold temperatures," *Applied Energy*, vol. 164, pp. 99–114, 2016.

[51] S. Al Hallaj, H. Maleki, J. S. Hong, and J. R. Selman, "Thermal modeling and design considerations of lithium-ion batteries," *Journal of Power Sources*, vol. 83, no. 1-2, pp. 1–8, 1999.

[52] C. R. Pals and J. Newman, "Thermal modeling of the lithium/polymer battery: I. Discharge behavior of a single cell," *Journal of the Electrochemical Society*, vol. 142, no. 10, pp. 3274–3281, 1995.

[53] Transport Simulation Systems, Aimsun, 2017, https://www.aimsun.com/.

[54] National oceanic and atmospheric administration, *National Centers for Environmental Information*, 2019, https://www.ncdc.noaa.gov/.

[55] Y. Li, Z. Wei, B. Xiong, and D. M. Vilathgamuwa, "Adaptive Ensemble-Based Electrochemical-Thermal Degradation State Estimation of Lithium-Ion Batteries," *IEEE Transactions on Industrial Electronics*, no. 69(7), pp. 6984–6996, 2022.

[56] H. Zhang, C. Li, H. Chen, and H. Fang, "Analysis of prismatic lithium-ion battery degradation based on an electrochemical-thermal-degradation model," *International Journal of Energy Research*, 2022.

[57] G. Zhao, X. Wang, and M. Negnevitsky, "Connecting battery technologies for electric vehicles from battery materials to management," *iScience*, vol. 25, no. 2, Article ID 103744, 2022.

[58] R. Mathieu, C. Martin, O. Briat, P. Gyan, and J.-M. Vinassa, "Comparative Ageing Study of CC-CV Fast Charging for Commercial 18650 Li-Ion Cells: Impact of Environmental Temperature," in *Proceedings of the 2019 IEEE Vehicle Power And Propulsion Conference (VPPC)*, pp. 1–5, IEEE, Hanoi, Vietnam, October 2019.